

Nodal Quasiparticle Lifetime in $\text{Bi}_2\text{Sr}_2\text{CaCu}_2\text{O}_{8+\delta}$

J. Corson, J. Orenstein

Materials Sciences Division, Lawrence Berkeley National Laboratory and Physics Department, University of California, Berkeley, California 94720

J. N. Eckstein

Department of Physics, University of Illinois, Urbana, Illinois 61801

(December 2, 2024)

We have measured the complex conductivity, σ , of a $\text{Bi}_2\text{Sr}_2\text{CaCu}_2\text{O}_{8+\delta}$ (BSCCO) thin film between 0.18 and 1.0 THz. We find σ in the superconducting state to be well described as the sum of contributions from quasiparticles, the condensate, and order parameter fluctuations which draw 30% of the spectral weight from the condensate. The quasiparticle scattering rate is approximately equal to $k_B T / \hbar$ above 20K.

74.25.Gz, 74.25.Nf, 74.25.-q, 74.72.Hs

The unusual properties of the quasiparticle lifetime τ_{qp} in high- T_c cuprate superconductors provide evidence for a non-fermi liquid normal state and a non-BCS mechanism. Because angle-resolved photoemission (ARPES) shows that the quasiparticle dispersion is highly anisotropic [1,2], it is important to distinguish the properties of τ_{qp} at different parts of the fermi surface. Near the $(\pi, 0)$ point in momentum space, where the maximum of the d-wave gap appears, the ARPES lineshape narrows dramatically upon cooling through T_c [1–3]. The change indicates the sudden onset of a well-defined quasiparticle in this antinodal region. Recently, improvements in detectors have made it possible to resolve the lineshape in the nodal or (π, π) direction as well. Valla *et al.* [4] reported that in the normal state, τ_{qp} can be described by the marginal fermi liquid phenomenology [5], $1/\tau_{qp} \sim \max(\omega, T)$. Surprisingly, they also found no change in this behavior upon cooling through T_c . This observation is currently controversial, as Kaminski *et al.* [6] report some changes in the lineshape near T_c which could indicate deviations from a marginal fermi liquid behavior. However, both groups agree that the change in nodal lineshape near T_c is less than that of the antinodal quasiparticles.

The nodal quasiparticle's apparent insensitivity to superconductivity is surprising for two reasons. First, one might expect the reduction in the phase space for scattering which accompanies the formation of a gap to increase the quasiparticle lifetime dramatically. Second, τ_{qp} determined by transport measurements in the closely related compound $\text{YBa}_2\text{Cu}_3\text{O}_{7-\delta}$ (YBCO) [7,8] does indeed increase rapidly below T_c . A microwave study of an extremely pure YBCO crystal measured essentially the entire Drude spectrum of the quasiparticle conductivity below 75 GHz [9]. From the width of the Drude peaks τ_{qp} was found to increase rapidly in the superconducting state, $\sim T^{-4}$ for $T \leq 60$ K [9]. Thermal transport measurements also indicate a sharp increase of τ_{qp} below T_c

[10].

Of course, transport experiments are not momentum resolved and they measure a fermi surface average of the quasiparticle lifetime. However, there is strong evidence that it is the nodal quasiparticle lifetime that is probed in the transport studies. It was reported in Ref. [9] that the complex conductivity, σ , can be described (at low T) by a two-fluid model which sums the contributions of condensate and quasiparticles. The spectral weight in the normal fluid, $\rho_n \sim \int \sigma_1 d\nu$, grows linearly with T at low temperature [9]. The rate of growth of $\rho_n(T)$ matches the linear decrease in superfluid density $\rho_s(T)$, measured independently via the penetration depth. The linear rate of transfer from ρ_s to ρ_n agrees with the theoretical prediction for nodal quasiparticles in a d-wave superconductor [11].

Thus, the transport measurements in YBCO stand in apparent contradiction to ARPES measurements in BSCCO. It would appear that either the single-particle lifetime probed by ARPES is qualitatively different than the transport lifetime, or YBCO and BSCCO are fundamentally different despite the similarity of their bilayer structure and T_c . The resolution of this issue requires interchanging the two probes and the two material systems. As it has proved difficult to obtain ARPES lineshapes in YBCO, it is important to focus on the transport properties of BSCCO.

Microwave data in BSCCO are quite different from those in YBCO. There is no discernable frequency dependence in σ_1 in the range from $\nu=10$ to 50 GHz [12–14]. Thus, the transport lifetime is not directly resolved in these measurements. They do indicate, however, that $1/\tau_{qp} \gg 2\pi \cdot 50$ GHz in BSCCO, a τ_{qp} much smaller than in YBCO. In addition, σ_1 in BSCCO single crystals rises to a broad peak near 25 K and does not decrease to zero. Even at the lowest temperatures measured, about 5 K, σ_1 remains 8 times the normal state value just above T_c , $\sigma_n(T_c)$, and is far larger than the "universal conductiv-

ity” proposed by Lee [15]. This stands in sharp contrast to $\rho_n \propto T$, as found in YBCO [9]. At the same time it is observed at low T that $\rho_s(T) = \rho_0 - \alpha T$ [12–14], indicating, as in YBCO [16], that the quasiparticles condense completely. The apparent contradiction, that the complete condensation of the quasiparticles is not accompanied by the disappearance of their spectral weight, suggests a problem with a two-fluid interpretation of the BSCCO data.

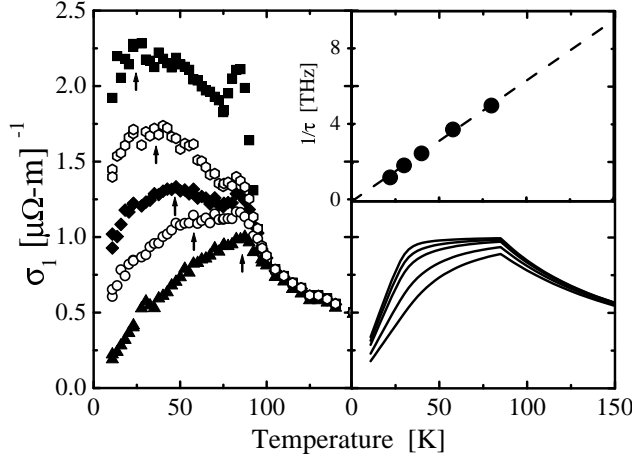


FIG. 1. Left panel: σ_1 plotted versus T for 0.2, 0.3, 0.4, 0.6 and 0.8 THz as squares, octagons, diamonds, circles and triangles. The arrows mark at each frequency the T where σ_1 begins its downturn. Upper right panel: $1/\tau_{qp}$ implied by the arrows plotted versus T , with the same T scale as the panel below. The dashed line is a fit to $1/\tau_{qp} \propto T$. Lower right panel: Drude conductivity, $\sigma_{qp}(T)$, using τ_{qp} proportional to the linear fit in the upper panel and $\rho_n = 4.8T$, plotted on the same scale as the left panel. The same frequencies are shown as the left panel, increasing ν having smaller $\sigma_{qp}(T)$.

In order to resolve this contradiction and to test the ARPES result that $1/\tau_{qp} \approx k_B T/\hbar$, we must look at higher frequencies, in the range $\hbar\nu \approx k_B T$. We present σ measured in a BSCCO thin film with a $T_c = 85K$, covering frequencies from 0.18 to 1.0 THz, above the range of microwave and below that of infrared spectroscopies. This high quality sample was grown on a lanthanum aluminate substrate using atomic layer-by-layer molecular beam epitaxy [17]. The resistance R versus T is linear and $R(0)/R(300K) = 4 \times 10^{-2}$ where $R(0)$ is the extrapolation of the linear resistance to zero temperature. We use coherent time-domain THz spectroscopy to measure both the real and imaginary parts of σ directly and independently [18]. Our data reveal a dramatic frequency dependence in σ below T_c . These are the first measurements in BSCCO to show a peak in $\sigma_1(T)$ which shifts with frequency. This observation allows us to determine τ_{qp} directly from our data. We find that above 20 K, $1/\tau_{qp}(T) \approx k_B T/\hbar$, in agreement with the recent ARPES data [4]. Below 20K, $1/\tau_{qp}$ appears to saturate at ≈ 2 THz. Furthermore, having identified the conductiv-

ity due to the normal fluid we find the total conductivity to be incompatible with a simple two-fluid model. Instead, we show the conductivity to be a combination of three contributions: quasiparticles, the condensate, and a low frequency collective mode with spectral weight drawn from the condensate.

We now turn to the σ_1 data and discuss its salient features. The left panel of Figure 1 shows σ_1 plotted versus temperature for a representative sample of frequencies in our range. At temperatures above T_c there is little frequency dependence, as we would expect since $1/\tau_{qp} \gg 2\pi \cdot 1$ THz in this temperature range. Below T_c , however, $\sigma_1(T)$ depends strongly on frequency. At $\nu=0.2$ THz we observe a behavior quite similar to that seen in the microwave data on BSCCO single crystals [12–14]. σ_1 rises to a maximum at 25 K, but remains much greater than $\sigma_n(T_c)$ at 5 K. As the frequency increases from 0.2 to 0.8 THz the maximum shifts from 25 K to nearly T_c , indicating that $1/\tau_{qp}$ is sweeping through our bandwidth. For a given frequency, the quasiparticle conductivity will decrease below the temperature where $1/\tau_{qp}(T) \approx \omega$. At each measurement frequency, this temperature is marked with an arrow. The measurement frequency (in radians/s) and corresponding T for each arrow are shown in the upper right panel of Fig. 1. This admittedly rough estimate clearly suggests a quasiparticle lifetime with the form $1/\tau_{qp} \sim T$. Finally, the peak in σ_1 near T_c , most visible at low frequencies, has been attributed to phase fluctuations of the order parameter due to thermal vortex, anti-vortex pairs [19].

Following its success in YBCO, we attempt to describe the conductivity using a two fluid model, in which σ below T_c is comprised of condensate and quasiparticle contributions. The condensate’s real, or dissipative, conductivity is a δ -function at $\nu = 0$. Therefore, for any nonzero frequency σ_1 is due solely to the quasiparticles. As found in YBCO, we choose a Drude conductivity for the quasiparticles, $\sigma_{qp}(\omega, T)/\sigma_Q \equiv (\rho_n \tau_{qp}/\hbar)/(1 + \omega^2 \tau_{qp}^2)$. Here $\sigma_Q \equiv e^2/(\hbar d)$ is the quantum conductivity of a stack of bilayers with spacing $d = 15.4\text{\AA}$. The spectral weight, ρ_n is expressed in units of energy as will be described below.

The two temperature dependent parameters, $\tau_{qp}(T)$ and $\rho_n(T)$ are clearly suggested by the data. The form of $\rho_n(T)$ follows from the T dependence of the superfluid density. We find $\rho_s(T)$ from the imaginary part of the conductivity, σ_2 , which is measured independently of σ_1 in our experiment. We observe that $\rho_s(T) = \rho_0 - \alpha T$ below about 30 K, suggesting that $\rho_n = \alpha T$ at low T . Because of the extreme anisotropy of BSCCO we convert the measured ρ_s to an areal density per CuO_2 bilayer. The areal superfluid density is the phase stiffness per bilayer, and can be conveniently expressed in thermal units of energy, or Kelvins. For this sample, $\rho_0 = 788$ K and $\alpha = 4.8$. For purposes of modeling, we have found that the most accurate description of the terahertz conductivity results if we assume that $\rho_n = \alpha T$ up to T_c , and is

constant for $T \geq T_c$.

Turning to $\tau_{qp}(T)$, the upper right panel of Fig. 1 suggests that $1/\tau_{qp} \sim T$ over a wide temperature range. The proportionality constant is set by the frequency-independent conductivity above T_c , $\sigma_n/\sigma_Q = \rho_n\tau_{qp}/\hbar = \alpha k_B T_c \tau_{qp}/\hbar$. This analysis yields $1/\tau_{qp}(T) = (0.97 \pm 0.1) k_B T/\hbar$.

In the right-hand panel of Fig. 1, we plot $\sigma_{qp}(T)$, the Drude conductivity with $\rho_n(T)$ and $\tau_{qp}(T)$ as described above. Above T_c , $\sigma_{qp}(T)$ accounts for all the dissipative conductivity. However, below T_c it is clear that this is no longer the case. Focusing first at the highest frequencies in our range, we see that $\sigma_{qp}(T)$ agrees rather well with the observed $\sigma_1(T)$. On the other hand, σ_1 at low temperature and frequency is dominated by an additional component.

To identify this component, it is instructive to consider the difference between the measured spectral weight and the amount that can be ascribed to quasiparticles. Figure 2 shows the spectral weight measured in our bandwidth, $\Sigma(T)$, and that due to the normal fluid, $\Sigma_{qp}(T)$, plotted versus temperature. These spectral weights denoted by Σ are distinct from those discussed earlier labeled with ρ 's. Whereas $\rho(T)$ represents an integration of σ_1 over all frequencies, $\Sigma(T)$ is confined to an integration over our experimental bandwidth. The difference between $\Sigma(T)$ and $\Sigma_{qp}(T)$ is plotted as triangles. It is apparent that $\Sigma_{qp}(T)$ is less than the total spectral weight observed. Notice that at low temperatures the difference, $\Sigma(T) - \Sigma_{qp}(T)$, is proportional to $\rho_s(T)$, shown here multiplied by 0.18. This remarkable fact, that the spectral weight of the conductivity not due to the quasiparticles is proportional to $\rho_s(T)$, is only true when we set $1/\tau_{qp}(T) \sim T$. If we choose $1/\tau_{qp}(T) \sim T^\beta$ with any β other than 1, the unaccounted for spectral weight does not have such a reasonable and recognizable temperature dependence.

The fact that the residual spectral weight is proportional to $\rho_s(T)$ suggests that it arises from fluctuations of the condensate order parameter. One example of dissipation due to such fluctuations is the narrow feature near T_c evident in Figs. 1 and 2. These fluctuations are associated with thermal excitation of vortex, anti-vortex pairs [19]. As T is lowered the population of such pairs falls exponentially. At low temperature there remain fluctuations of small amplitude, whose conductivity is expected to be of order σ_Q or $\sim 1.6 \times 10^5 (\Omega^{-1} - m^{-1})$ [20], which is far too small to explain the data. However, the situation can be quite different in the presence of static (or quasi-static) spatial variation in the superfluid density. Two examples have been discussed recently in the literature. The first is a one-dimensional periodic modulation of the phase-stiffness parameter [21]. The second example is a "granular" superconductor in which the Josephson coupling between grains is randomly distributed about its mean value [22]. Both of these models predict a contribution to σ_1 above zero frequency which is not present if

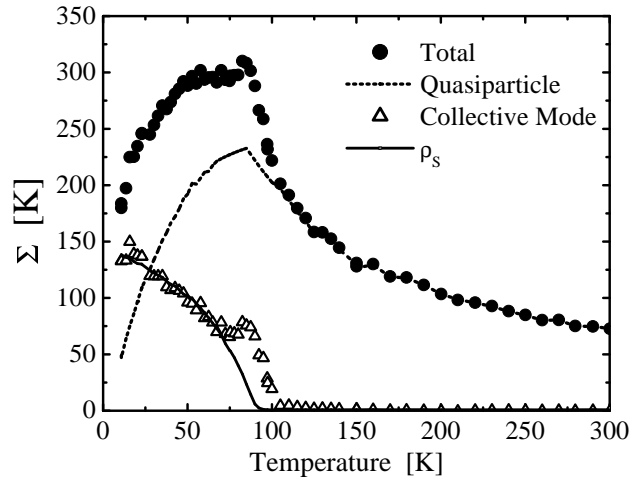


FIG. 2. The spectral weight in our bandwidth (0.2-0.8 THz) of the total conductivity, $\Sigma(T)$, the quasiparticle Drude conductivity, $\Sigma_{qp}(T)$, and the difference between the two, $\Sigma(T) - \Sigma_{qp}(T)$, plotted versus temperature as circles, a dotted line and triangles, respectively. The solid line shows the superfluid density, $\rho_s(T)$, multiplied by 0.18, to show the proportionality between this and the portion of the spectral weight not due to the quasiparticles.

the phase stiffness is homogeneous throughout the material. Moreover, the spectral weight in this new contribution to σ_1 is proportional to the mean value of the phase stiffness, or superfluid density, just as is observed in our experiments. In both cases the proportionality constant is $(\Delta\rho_s)^2/\bar{\rho}_s^2$, the fractional mean square variation in ρ_s .

Motivated by these models, we attempt a decomposition of σ_1 into quasiparticle and collective mode (CM) contributions, $\sigma_1 \equiv \sigma_{qp} + \sigma_{cm}$. The difference between the measured σ_1 and σ_{qp} shows that the collective mode contribution is a low frequency peak contained, predominately, within our frequency range. We therefore test this decomposition with σ_{cm} chosen to be a Lorentzian centered at $\nu = 0$. This introduces two collective mode parameters: width, $\Gamma_{cm}(T)$, and spectral weight, $\rho_{cm}(T)$. As is suggested by Fig. 2 we set the spectral weight of the collective mode, $\rho_{cm}(T)$, equal to a fixed fraction, κ , of $\rho_s(T)$. For the spectral weight of the normal fluid we choose $\rho_n = \alpha T$ as before. At every temperature, we vary both Γ_{cm} and τ_{qp} in order to find the best fit to the data. We find $1/\tau_{qp}(T) \approx k_B T/\hbar$ down to 20K where it appears to saturate at a value near 2 THz. The width of the collective mode is found to be temperature independent within the noise level, with a value 1.5 THz, and $\kappa = 0.30$.

The left panel of Figure 3 compares $\sigma_1(T) - \sigma_{qp}(T)$ with $\sigma_{cm}(T)$, obtained using the parameter values given above. At each frequency $\sigma_1(T) - \sigma_{qp}(T)$ is plotted as symbols and $\sigma_{cm}(T)$ is shown as a solid line. The difference between σ_1 and σ_{qp} is obviously well described by the collective mode. What deviation there is between the model and the data is shown in the bottom right panel

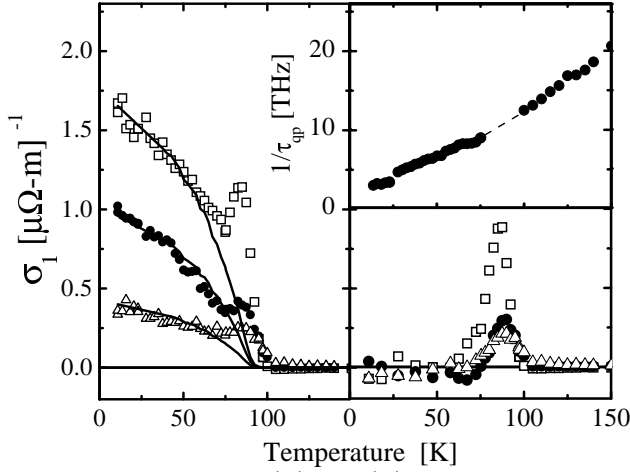


FIG. 3. Left panel: $\sigma_1(T) - \sigma_{qp}(T)$ plotted at 0.2, 0.36 and 0.64 THz as squares, circles and triangles, respectively. The lines show $\sigma_{cm}(T)$ from our model. Lower right panel: The difference between the data and the fit are plotted on the same scale as the left panel, and are ascribed to thermal phase fluctuations. Upper right panel: $1/\tau_{qp}(T)$ for the quasiparticles, due to this same model, plotted versus temperature with the T scale given by the panel below.

of Fig. 3. We see that difference corresponds to the phase fluctuations near T_c . The temperature dependent quasiparticle lifetime which best fits the data is shown in the upper right panel of Fig. 4. While it is clear that $1/\tau_{qp}(T)$ shows some deviation from linear in T , it is equally clear that there is no dramatic lengthening of $\tau_{qp}(T)$ at T_c . The dashed line between 75-100 K indicates the range where the large thermal fluctuation conductivity dominates the quasiparticle contribution, making it difficult to extract τ_{qp} .

At this point we comment briefly on the frequency dependence of the collective mode conductivity. In both models described previously, the frequency of the collective mode is related to the screened plasma frequency of the condensate, or $\hbar\omega_p = \sqrt{\rho_s e^2 / \epsilon d}$. With $\epsilon \sim 10$, this yields $\hbar\omega_p \sim 1400$ K, much higher than the energies probed in our experiment. However, the plasma mode can be strongly perturbed by thermal quasiparticles. For example, the damping rate of the plasmon, Γ , is given by $\hbar\Gamma = \rho_s \sigma_Q / \sigma_{qp}$. For the values of σ_{qp} seen in our experiment, this is of order 100 K, indicating that the plasma mode is highly overdamped. The corresponding conductivity will be centered at $\nu = 0$ and its width will depend on the damping and screening effects of the quasiparticle background.

One final observation concerning our data is that causality dictates that the collective mode feature in $\sigma_1(\nu)$ must also be clearly manifest in $\sigma_2(\nu)$. Since both σ_1 and σ_2 are measured directly and independently by our coherent spectroscopy this is an important check of our model's description of the conductivity. We find the total $\sigma_2(\nu)$ to be a sum of contributions from the quasi-

particles, the condensate and the collective mode. $\sigma_2(\nu)$, therefore, is not described by a two fluid model but instead is well described by the model set forth above.

We have shown that the dissipative conductivity of BSCCO in the superconducting state is not due solely to a normal fluid of quasiparticles. There is clearly an additional contribution whose spectral weight increases with decreasing temperature. We describe this contribution as a Lorentzian whose width is temperature independent and whose spectral weight is a constant fraction of $\rho_s(T)$. Adding this contribution to the conductivity of nodal quasiparticles with $1/\tau_{qp} \sim T$ successfully describes the complex features of σ over the entire experimental range of frequency and temperature.

We thank D.H. Lee, A. Maeda and D. Stroud for helpful discussions. This work was supported under NSF Grant No. 9870258, DOE Contract No. DE-AC03-76SF00098, and ONR Contract No. N00014-94-C-001.

-
- [1] Z.-X. Shen and D. S. Dessau, Phys. Rep. **253**, 1 (1995).
 - [2] J. C. Campuzano *et al.*, in *The Gap Symmetry and Fluctuations in High- T_c Superconductors*, eds. J. Bok *et al.* (Plenum, New York, 1998), p. 229.
 - [3] A. V. Fedorov *et al.*, Phys. Rev. Lett. **82**, 2179 (1999).
 - [4] T. Valla *et al.*, Science **285**, 2110 (1999).
 - [5] C. M. Varma *et al.*, Phys. Rev. Lett. **63**, 1996 (1989).
 - [6] A. Kaminski *et al.*, Phys. Rev. Lett. **84**, 1788 (2000).
 - [7] M. C. Nuss *et al.*, Phys. Rev. Lett. **66**, 3305 (1991).
 - [8] D. A. Bonn, P. Dosanjh, R. Liang, and W. N. Hardy, Phys. Rev. Lett. **68**, 2390 (1992).
 - [9] A. Hosseini *et al.*, Phys. Rev. B **60**, 1349 (1999).
 - [10] N. P. Ong, K. Krishana, Y. Zhang and Z. A. Xu, preprint, cond-mat/9904160.
 - [11] J. Annett, N. Goldenfeld and S. R. Renn, Phys. Rev. B **43**, 2778 (1991).
 - [12] T. Jacobs *et al.*, Phys. Rev. Lett. **75**, 4516 (1995).
 - [13] S.-F. Lee *et al.*, Phys. Rev. Lett. **77**, 735 (1996).
 - [14] H. Kitano *et al.*, J. Low Temp. Phys. **117**, 1241 (1999).
 - [15] P. A. Lee, Phys. Rev. Lett. **71**, 1887 (1993).
 - [16] W. N. Hardy *et al.*, Phys. Rev. Lett. **70**, 3999 (1993).
 - [17] J. N. Eckstein and I. Bozovic, Annu. Rev. Mat. Sci. **25**, 679 (1995).
 - [18] M. C. Nuss and J. Orenstein, in *Millimeter and Submillimeter Spectroscopy of Solids*, ed. G. Grüner (Springer, New York, 1998), p. 7.
 - [19] J. Corson *et al.*, Nature **398**, 221 (1999).
 - [20] S. Sachdev and O. A. Starykh, pre-print, cond-mat/9904354.
 - [21] D. van der Marel and A. Tsvetkov, Czech. J. Phys. **46**, 3165 (1996).
 - [22] S. Barabash, D. Stroud and I.-J. Hwang, preprint, cond-mat/0002346.